Entanglement-Enhanced Atomic Gravimeter

Christophe Cassens[1,2,*] Bernd Meyer-Hoppe[1,2] Ernst Rasel,[1] and Carsten Klempt[1,2]

[1]*Leibniz Universität Hannover, Institut für Quantenoptik, Welfengarten 1, D-30167 Hannover, Germany*
[2]*Deutsches Zentrum für Luft- und Raumfahrt e.V. (DLR),*
Institut für Satellitengeodäsie und Inertialsensorik, Callinstraße 30b,
D-30167 Hannover, Germany

Interferometers based on ultracold atoms enable an absolute measurement of inertial forces with unprecedented precision. However, their resolution is fundamentally restricted by quantum fluctuations. Improved resolutions with entangled or squeezed atoms were demonstrated in internal-state measurements for thermal and quantum-degenerate atoms and, recently, for momentum-state interferometers with laser-cooled atoms. Here, we present a gravimeter based on Bose-Einstein condensates with a sensitivity of $-1.7_{-0.5}^{+0.4}$ dB beyond the standard quantum limit. Interferometry with Bose-Einstein condensates combined with delta-kick collimation minimizes atom loss in and improves scalability of the interferometer to very-long-baseline atom interferometers.

Atom interferometers, in particular, light-pulse interferometers, are employed for sensing gravitational fields, with applications for gravimetry [1], gradiometry [2–5], tests of general relativity [6–8], and the detection of gravitational waves [9–17]. The resolution of the gravity signal is ideally bounded by the standard quantum limit (SQL) that scales with the square root of the atom number. Increasing the flux of ultracold atoms is a challenge, and, moreover, quantum density fluctuations eventually limit the achievable resolution [18]. These limits can be overcome by operating the interferometers with squeezed atomic input states, where entanglement between the atoms enables a suppression of these fundamental signal fluctuations.

Squeezing-enhanced sensitivities were demonstrated in a wide variety of systems [19] but mainly in internal degrees of freedom that do not couple to inertial forces. Entanglement of momentum modes was generated with colliding atoms [20–22] and in our previous work using atomic Bose-Einstein condensates (BECs) [23]. Proof-of-principle demonstrations of spin-squeezed Mach-Zehnder interferometers are so far based on laser-cooled atoms [24,25]. The retrieval of a gravitational signal was not yet reported. Moreover, high-precision gravimetry scenarios

benefit from Bose-Einstein condensed atomic ensembles, because the obtainable narrower position and velocity distributions [26] suppress systematic uncertainties [18]. In addition, the small cloud size and velocity width enable a large momentum transfer despite wavefront distortions and the stringent velocity selectivity, respectively [27–29]. A further application of BEC interferometry could be gravimetry at small distances, where small cloud sizes and low densities favor an entanglement enhancement. The development of a BEC-based squeezing concept for gravimetry is, therefore, highly desirable [30,31].

Here, we report the application of squeezed states in rubidium BECs to measure the gravitational acceleration with a sensitivity beyond the SQL. Two-mode squeezing is generated by spin-changing collisions and transferred to single-mode squeezing on the magnetic-field-insensitive clock transition. Microwave (mw) and Raman-laser pulses are combined to form a gravity-sensitive atom interferometer. The input state with $-5.4_{-0.5}^{+0.4}$ dB spin squeezing enables an interferometer operation with a sensitivity of $-3.9_{-0.7}^{+0.6}$ dB below the experimentally recorded coherent-state reference and $-1.7_{-0.5}^{+0.4}$ dB below the theoretical SQL. An alternating operation of two interferometer sequences with different interrogation times yields an absolute measurement of the gravitational acceleration. Our concept can be implemented in existing large-scale BEC-based atom interferometers with small integration efforts.

We initially create BECs of 6×10^3 ^{87}Rb atoms in a crossed-beam optical dipole trap with trapping frequencies $2\pi \times \{150, 160, 220\}$ Hz. The atoms are prepared in spin

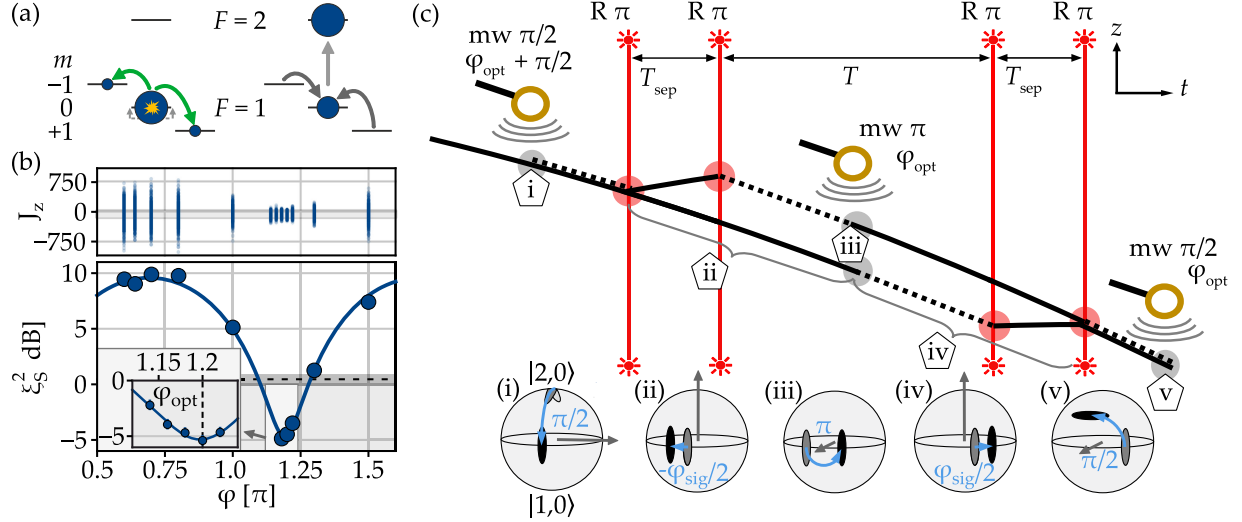*Contact author: Christophe.Cassens@dlr.de

FIG. 1. The entanglement-enhanced gravimeter. (a) Generation of two-mode squeezing by spin-changing collisions (green) via mw dressing, followed by a transfer to clock states via mw (light gray) and rf (dark gray) pulses. (b) Spin-noise tomography of the interferometer input state. The upper graph shows the normalized population in $|2,0\rangle$ depending on the scanned mw phase φ with blue dots as individual measurements. In the bottom graph, the variance of these data points is compared to the SQL yielding a spin-squeezing parameter ξ_S^2. The inset shows a detailed measurement around the minimum that represents the optimal squeezing angle φ_{opt} (dashed line). The solid blue line presents a sinusoidal fit to the data, the dashed black line and gray area the experimental coherent state with $0.5_{-0.5}^{+0.4}$ dB, and the hatched area the spin-squeezed regime with sub-SQL fluctuations. Error bars of squeezing parameters are the statistical ± 1 standard error [32] but are smaller than the marker size. (c) Interferometric sequence in a space-time diagram (top) and in Bloch-sphere representation (bottom). Dashed lines indicate the hyperfine level $|1,0\rangle$ and solid lines $|2,0\rangle$. Hyperfine levels are changed by mw and Raman (R) pulses. Raman pulses also induce a state-dependent change in momentum mode. For the Bloch spheres, blue arrows indicate rotations and gray arrows the respective rotation axes. The north pole corresponds to $|2,0\rangle$ and the south pole to $|1,0\rangle$. The squeezed input state is rotated into the phase-squeezed direction (i) and senses a phase φ_{sig} (ii)–(iv) that is finally mapped onto a population imbalance for readout (v).

level $|F,m\rangle = |1,0\rangle$ in a homogeneous magnetic field of 90 μT that is actively stabilized within ± 7 nT and oriented in parallel to Earth's gravitational field. Because of the quadratic Zeeman shift, the creation of pairs of atoms in $|1,\pm 1\rangle$ caused by spin-changing collisions [32,33] is, in principle, prevented. We activate this spin dynamics by dressing the clock transition ($|1,0\rangle \leftrightarrow |2,0\rangle$) with a blue-detuned mw field for 50 ms, thus compensating the quadratic Zeeman shift. This populates the levels $|1,\pm 1\rangle$ with a two-mode squeezed vacuum state [Fig. 1(a), left] according to the Hamiltonian [34]

$$\hat{H} = \hat{H}_a - \hat{H}_s \tag{1}$$

with

$$\hat{H}_{s/a} = \frac{\Omega}{2}(\hat{a}_{s/a}\hat{a}_{s/a} + \hat{a}_{s/a}^\dagger\hat{a}_{s/a}^\dagger). \tag{2}$$

The Hamiltonian contains pairs of the operators

$$\hat{a}_{s/a}^{(\dagger)} = \frac{1}{\sqrt{2}}(\hat{a}_{+1}^{(\dagger)} \pm \hat{a}_{-1}^{(\dagger)}) \tag{3}$$

which create and annihilate pairs of atoms in the symmetric (s) and antisymmetric (a) superposition of the levels $|1,\pm 1\rangle$. We measure a spin dynamics interaction strength of $\Omega = h \times 3.77$ Hz. The experimental sequence continues by switching off the dipole trap, such that density-dependent interactions cease. After 1 ms of free fall, the dipole trap is turned on again for 350 μs in order to slow down the expansion of the cloud [23,35]. Up to this point, the spin-squeezed state is magnetic-field sensitive to first order. To transfer the squeezed vacuum in $|1,\pm 1\rangle$ to a magnetically insensitive clock state, the large amount of atoms in $|1,0\rangle$ is first transferred to $|2,0\rangle$ by a mw π pulse. Atoms in $|1,\pm 1\rangle$ are then transferred to $|1,0\rangle$ by a σ^--polarized radio-frequency (rf) π pulse with phase ϕ_{rf} [Fig. 1(a), right] that leaves the atoms in $F = 2$ unaffected [36]. The rf pulse couples only to the symmetric superposition and, thus, transfers a single-mode squeezed state to $|1,0\rangle$, containing on average 1.9 atoms [37]. The few remaining atoms in the levels $|1,\pm 1\rangle$ do not contribute to the interferometer sequence. The combination of the single-mode squeezed vacuum state in $|1,0\rangle$ and the large number of atoms in $|2,0\rangle$ constitutes a spin-squeezed state as a basis for the entanglement-enhanced gravimeter described below. For the final detection of the interferometer output,

we separate Zeeman levels with different m by a strong magnetic-field gradient and employ absorption detection [37].

Before the description of the gravimeter, we present a characterization of the single-mode spin-squeezed state in a spin-noise-tomography measurement [19] based on mw pulses on the clock transition with Rabi frequency $\Omega_{\text{mw}} = 2\pi \times 20.9$ kHz and duration τ. The population imbalance

$$J_z = \frac{1}{2} \ (N_{F=2} - N_{F=1}) \tag{4}$$

is recorded after a spin-echo sequence. This sequence consists of three mw pulses of type $(\pi/2)_{\varphi+\pi/2}, (\pi)_\varphi$, $(\pi/2)_\varphi$, where θ_ϕ specifies the mw pulse by $\theta = \Omega_{\text{mw}}\tau$ and the adjustable mw phase ϕ. Figure 1(b) shows fluctuations of J_z as a function of the scanned mw phase φ with respect to the rf phase ϕ_{rf}. From the variance of the measured data at each phase, we obtain a spin-squeezing parameter [19] of

$$\xi_S^2 = 4 \frac{\text{Var}(J_z)}{N} \hat{=} - 5.4^{+0.4}_{-0.5} \ \text{dB} \tag{5}$$

at a mw phase of $\varphi_{\text{opt}} = 1.2\pi$. The corresponding anti-squeezing amounts to $9.9^{+0.4}_{-0.5}$ dB at $\varphi_{\text{opt}} + (\pi/2)$. This spin-squeezed state is insensitive to magnetic-field fluctuations to first order and subsequently employed to decrease the quantum noise in an inertially sensitive interferometer sequence.

The interferometric measurement [Fig. 1(c)] is now a combination of the spin-echo sequence from above (i),(iii), (v) with four Raman-laser pulses that form a gravity-sensitive Mach-Zehnder interferometer. It starts by applying a mw $\pi/2$ pulse with a phase $\varphi_{\text{opt}} + (\pi/2)$. In this orientation, the state features a minimal uncertainty of the phase between the two clock states (i). After 1.9 ms, a Raman π pulse driving the transition $|1, 0; p = 0\rangle \rightarrow |2, 0; p = \hbar k_{\text{eff}}\rangle$ with 98.1(7)% efficiency renders the interferometer sensitive to acceleration (ii). The Raman pulse transfers two-photon momenta $\hbar k_{\text{eff}} = 1.18 \ (\text{cm/2}) \times m_{\text{Rb-87}}$ with $m_{\text{Rb-87}}$ being the atomic mass, leading to a spatial delocalization of the two momentum modes. A description and characterization of the Raman laser system can be found in Supplemental Material [37]. The $\tau_R = 60$-µs-long Raman pulse is Blackman shaped [38] to suppress the unwanted transition $|2, 0; p = 0\hbar k_{\text{eff}}\rangle$ to $|1, 0; p = -\hbar k_{\text{eff}}\rangle$, which is only $2\pi \times 30$ kHz detuned. The two clouds separate for $T_{\text{sep}} = 77$ µs before a second Raman π pulse decelerates the upper arm of the interferometer by driving the same transition. While the two clouds fall in the same momentum mode for a time T, the internal states are inverted by a resonant mw π pulse to echo the spin evolution and suppress common noise like differential ac-Stark shifts, mw and Raman phase noise, and systematic mw frequency offsets (iii). After the inverting echo pulse, the two

arms acquire an additional gravitational phase shift, now with opposite sign (iv), such that it is not canceled by the echo sequence. The clouds are reunited by performing the identical Raman processes on the lower arm of the interferometer. 1.9 ms after the mw π pulse, the imprinted inertial phase with squeezed quantum noise is mapped onto the population imbalance J_z by a mw $\pi/2$ pulse with phase φ_{opt} (v). The time between the final Raman and the closing mw pulse allows additional parasitic interferometer paths, that arise from incomplete Raman transfers, to detach from the main paths.

The frequency difference of the Raman laser beams is switched between the pulses according to a frequency chirp rate which is varied around the value $\alpha = 9.8126 \ \text{m/s}^2 \times k_{\text{eff}}$. This frequency chirp counteracts the gravitational phase $g \times k_{\text{eff}}$ perceived by the freely falling atoms, yielding a recorded phase signal of

$$\varphi_{\text{sig}} = \left(g - \frac{\alpha}{k_{\text{eff}}} \right) S(T, T_{\text{sep}}, \tau_R). \tag{6}$$

Here, g is the gravitational acceleration of the atoms, and S is a scale factor depending on the interferometer geometry and the Raman pulse duration and shape [39].

If the chirp rate is set to exactly cancel the gravitational shift, the imprinted inertial phase vanishes according to Eq. (6) for all scaling factors. By choosing a phase difference of $\pi/2$ between the opening and closing mw $\pi/2$ pulses, the accumulated phase maps to a measurement of $J_z = 0$ (midfringe position). Figure 2(a) shows the normalized population in $F = 2$ for three different durations T. From the interception of the curves, an approximate value for the compensating chirp rate and a corresponding working range can be extracted.

The determination of the gravitational acceleration and the entanglement-enhanced sensitivity is performed by an alternating measurement of the normalized population in $F = 2$ for two different durations $T_1 = 455$ µs and $T_2 = 155$ µs at the previously determined chirp rate. This alternating operation suppresses the influence of drifts of the Raman pulse efficiencies that are slow with respect to the cycle time of 52 s. Since the scale factors and the corresponding slopes at this point differ, an experimental value for the gravitational acceleration g_{exp} can be obtained from the difference

$$\delta p = p(T_1) - p(T_2) = \frac{N_{F=2}(T_1)}{N(T_1)} - \frac{N_{F=2}(T_2)}{N(T_2)} \tag{7}$$

of the normalized populations of $|F = 2\rangle$ [see Fig. 2(a), inset] according to

$$g_{\text{exp}} = \frac{2}{C} \frac{\delta p}{S(T_1) - S(T_2)} + \frac{\alpha}{k_{\text{eff}}} \tag{8}$$
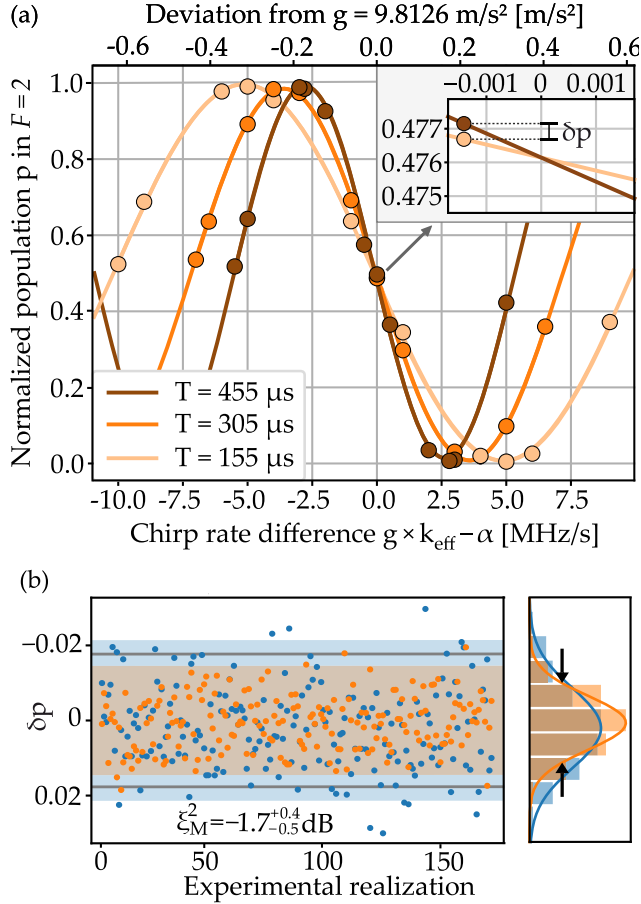
FIG. 2. Contrast and midfringe measurement. (a) Interferometer fringes for three different times T of the squeezed gravimeter depicted in Fig. 1(c) over chirp rate α. From the sinusoidal fits, we infer a contrast of 98.0(1.4)%. All interferometer fringes intercept for the chirp rate which compensates the gravitational acceleration of the atoms in accordance with Eq. (6). The standard deviation of the measurements is smaller than the markers. The inset enlarges the crossing region from which the local gravitation g_{exp} is obtained by a measurement of the difference signal δp. (b) Gravimetry signal δp as interferometer output. The gravimeter signal of the squeezing-enhanced operation (orange) has reduced fluctuations compared to the operation with a coherent state (blue). Experimentally, we achieve a metrologically relevant reduction of the variance of $-3.9^{+0.6}_{-0.7}$ dB compared to the experimentally recorded coherent input state and $\xi_M^2 = -1.7^{+0.4}_{-0.5}$ dB compared to the theoretical SQL. Shaded areas indicate ± 2 standard deviations of the respective data, gray lines ± 2 standard deviations corresponding to the SQL.

with contrast $C = 98.0(1.4)\%$ obtained from the full fringes in Fig. 2(a) and respective scale factors $S(T_1) = -1.42(1)$ s/m^2 and $S(T_2) = -0.767(3)$ s/m^2. The measured value of $g_{\mathrm{exp}} = 9.8118(16)$ m/s^2 agrees with the local gravitational acceleration of 9.812637196(88) m/s^2 [44] within the bounds of one standard error. Note that the error of the scale factors contributes much less to
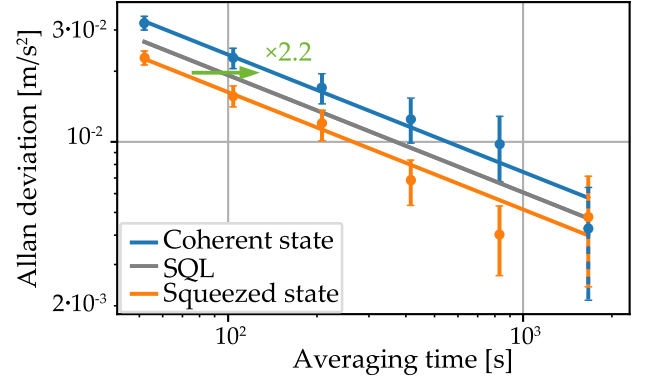

FIG. 3. Allan deviation of the gravimeter sequence using coherent states (blue) and squeezed states (orange). The squeezing-enhanced sequence reaches any instability 1.4 times faster than the theoretical optimum at the SQL (gray line) and 2.2 times faster than the experimentally recorded equivalent with coherent states. The technical noise sources for both sequences are the same. Error bars are the statistical ± 1 standard error [45].

the uncertainty in g_{exp} than the statistical uncertainty. Furthermore, the scale factors inferred from the fringe measurements are reproduced by the theoretical calculation [37].

We evaluate the metrological improvement by comparing the recorded measurement fluctuations with the optimal result from an ideal unentangled coherent state. We obtain a metrological squeezing factor

$$\xi_M^2 = \frac{4}{C^2} \frac{\mathrm{Var}[J_z(T_1) - J_z(T_2)]}{N(T_2) + N(T_1)} \triangleq -1.7^{+0.4}_{-0.5} \text{ dB}, \quad (9)$$

where $[N(T_2) + N(T_1)]/4$ is the SQL of the difference of two independent measurements with their respective atom numbers $N(T_2)$ and $N(T_1)$. This improvement proves the entanglement-enhanced measurement of the gravitational acceleration and constitutes the main result of our work. The corresponding data are shown in Fig. 2(b) in comparison to a coherent state realization.

We further analyze the temporal behavior throughout the measurement runs by calculating the Allan deviations [45] of δp for a coherent and a squeezed input state shown in Fig. 3. The coherent-state case is realized by omitting the squeezing generation section in the original experimental sequence. The squeezed-state results outperform the coherent-state equivalent over the whole range of averaging times. From a fit to the first 800 s of averaging time, we conclude that the squeezed-state signal averages down 2.2 times faster than the coherent-state signal and 1.4 times faster than the SQL for the same number of employed atoms.

In summary, we have presented a concept for enhancing atomic gravimeters beyond the SQL. Our demonstration involves all components for a large-scale implementation aiming for highest sensitivities. The squeezing method can be implemented in existing BEC-based atomic sources and

can be scaled to large atom numbers due to the utilization of vacuum squeezing. The measured antisqueezing is lower compared to other squeezing protocols like cavity-quantum nondemolition measurement and helps to maintain a large contrast and dynamical range in the interferometry signal. The implementation with BECs provides low expansion velocities and exquisite control of the spatial mode to suppress systematic effects due to laser wavefront curvature and distortion or Coriolis force [46]. We have shown that the squeezing is compatible with a further delta-kick reduction of the expansion velocity as required for long interrogation times. The squeezing angle can be freely adjusted and enables the anticipation and suppression of density-dependent quantum fluctuations [18].

The observed reduction of the squeezing due to the interferometer sequence stems solely from technical noise of the Raman laser system which constitutes an independent task for reaching highest sensitivities. Compared to conventional Mach-Zehnder interferometers, our concept features equal spin states during separation and recombination, suppressing the sensitivity to light shifts, mw shifts, and magnetic-field noise.

Our method recommends itself for differential measurements, as performed in gradiometry, tests of the universality of free fall, or gravitational wave detection. In such configurations, technical noise, e.g., induced by vibrations, is common mode and cancels, enabling the exploitation of entanglement enhancement. We envision the application of entanglement-enhanced interferometry at much increased interrogation times, either in large-scale fountains like the Very-Long-Baseline Atom Interferometer [47] or in micro-gravity environments like the Einstein Elevator [48]. The latter is currently pioneered by the INTENTAS [49] project, which aims at demonstrating an entanglement enhancement for future space-borne high-precision atom interferometers. Further applications include measurements of fundamental constants [50–52] as well as tests of classicalization [53].

The authors declare no competing interests.

Data availability

The data that support the findings of this article are openly available [54].

[1] J. M. McGuirk, M. J. Snadden, and M. A. Kasevich, *Large area light-pulse atom interferometry*, Phys. Rev. Lett. **85**, 4498 (2000).

[2] P. Asenbaum, C. Overstreet, T. Kovachy, D. D. Brown, J. M. Hogan, and M. A. Kasevich, *Phase shift in an atom interferometer due to spacetime curvature across its wave function*, Phys. Rev. Lett. **118**, 183602 (2017).

[3] S.-W. Chiow, J. Williams, N. Yu, and H. Müller, *Gravity-gradient suppression in spaceborne atomic tests of the equivalence principle*, Phys. Rev. A **95**, 021603(R) (2017).

[4] G. W. Biedermann, X. Wu, L. Deslauriers, S. Roy, C. Mahadeswaraswamy, and M. A. Kasevich, *Testing gravity with cold-atom interferometers*, Phys. Rev. A **91**, 033629 (2015).

[5] J. M. McGuirk, G. T. Foster, J. B. Fixler, M. J. Snadden, and M. A. Kasevich, *Sensitive absolute-gravity gradiometry using atom interferometry*, Phys. Rev. A **65**, 033608 (2002).

[6] S. Dimopoulos, P. W. Graham, J. M. Hogan, and M. A. Kasevich, *Testing general relativity with atom interferometry*, Phys. Rev. Lett. **98**, 111102 (2007).

[7] S. Dimopoulos, P. W. Graham, J. M. Hogan, and M. A. Kasevich, *General relativistic effects in atom interferometry*, Phys. Rev. D **78**, 042003 (2008).

[8] C. Ufrecht, F. Di Pumpo, A. Friedrich, A. Roura, C. Schubert, D. Schlippert, E. M. Rasel, W. P. Schleich, and E. Giese, *Atom-interferometric test of the universality of gravitational redshift and free fall*, Phys. Rev. Res. **2**, 043240 (2020).

[9] S. Abend *et al.*, *Terrestrial very-long-baseline atom interferometry: Workshop summary*, AVS Quantum Sci. **6**, 024701 (2024).

[10] M. Abe, P. Adamson, M. Borcean, D. Bortoletto, K. Bridges, S. P. Carman, S. Chattopadhyay, J. Coleman, N. M. Curfman, K. DeRose *et al.*, *Matter-wave atomic gradiometer interferometric sensor (MAGIS-100)*, Quantum Sci. Technol. **6**, 044003 (2021).

[11] L. Badurina, E. Bentine, D. Blas, K. Bongs, D. Bortoletto, T. Bowcock, K. Bridges, W. Bowden, O. Buchmueller, C. Burrage *et al.*, *AION: An atom interferometer observatory and network*, J. Cosmol. Astropart. Phys. 05 (2020) 011.

[12] B. Canuel *et al.*, *ELGAR—A European laboratory for gravitation and atom-interferometric research*, Classical Quantum Gravity **37**, 225017 (2020).

[13] G. M. Tino *et al.*, *SAGE: A proposal for a space atomic gravity explorer*, Eur. Phys. J. D **73**, 228 (2019).

[14] B. Canuel *et al.*, *Exploring gravity with the MIGA large scale atom interferometer*, Sci. Rep. **8**, 14064 (2018).

[15] J. M. Hogan and M. A. Kasevich, *Atom-interferometric gravitational-wave detection using heterodyne laser links*, Phys. Rev. A **94**, 033632 (2016).

[16] J. M. Hogan, D. M. S. Johnson, S. Dickerson, T. Kovachy, A. Sugarbaker, S.-w. Chiow, P. W. Graham, M. A. Kasevich, B. Saif, S. Rajendran *et al.*, *An atomic gravitational wave*

interferometric sensor in low earth orbit (AGIS-LEO), Gen. Relativ. Gravit. **43,** 1953 (2011).

[17] S. Dimopoulos, P. W. Graham, J. M. Hogan, M. A. Kasevich, and S. Rajendran, *Atomic gravitational wave interferometric sensor*, Phys. Rev. D **78,** 122002 (2008).

[18] P. Feldmann, F. Anders, A. Idel, C. Schubert, D. Schlippert, L. Santos, E. M. Rasel, and C. Klempt, *Optimal squeezing for high-precision atom interferometers*, arXiv:2311.10241.

[19] L. Pezzè, A. Smerzi, M. K. Oberthaler, R. Schmied, and P. Treutlein, *Quantum metrology with nonclassical states of atomic ensembles*, Rev. Mod. Phys. **90,** 035005 (2018).

[20] M. Bonneau, J. Ruaudel, R. Lopes, J.-C. Jaskula, A. Aspect, D. Boiron, and C. I. Westbrook, *Tunable source of correlated atom beams*, Phys. Rev. A **87,** 061603(R) (2013).

[21] P. Dussarrat, M. Perrier, A. Imanaliev, R. Lopes, A. Aspect, M. Cheneau, D. Boiron, and C. I. Westbrook, *Two-particle four-mode interferometer for atoms*, Phys. Rev. Lett. **119,** 173202 (2017).

[22] R. Bücker, J. Grond, S. Manz, T. Berrada, T. Betz, C. Koller, U. Hohenester, T. Schumm, A. Perrin, and J. Schmiedmayer, *Twin-atom beams*, Nat. Phys. **7,** 608 (2011).

[23] F. Anders, A. Idel, P. Feldmann, D. Bondarenko, S. Loriani, K. Lange, J. Peise, M. Gersemann, B. Meyer-Hoppe, S. Abend *et al.*, *Momentum entanglement for atom interferometry*, Phys. Rev. Lett. **127,** 140402 (2021).

[24] B. K. Malia, Y. Wu, J. Martínez-Rincón, and M. A. Kasevich, *Distributed quantum sensing with mode-entangled spin-squeezed atomic states*, Nature (London) **612,** 661 (2022).

[25] G. P. Greve, C. Luo, B. Wu, and J. K. Thompson, *Entanglement-enhanced matter-wave interferometry in a high-finesse cavity*, Nature (London) **610,** 472 (2022).

[26] C. Deppner, W. Herr, M. Cornelius, P. Stromberger, T. Sternke, C. Grzeschik, A. Grote, J. Rudolph, S. Herrmann, M. Krutzik *et al.*, *Collective-mode enhanced matter-wave optics*, Phys. Rev. Lett. **127,** 100401 (2021).

[27] S.-W. Chiow, T. Kovachy, H.-C. Chien, and M. A. Kasevich, *102ℏk large area atom interferometers*, Phys. Rev. Lett. **107,** 130403 (2011).

[28] J. E. Debs, P. A. Altin, T. H. Barter, D. Döring, G. R. Dennis, G. McDonald, R. P. Anderson, J. D. Close, and N. P. Robins, *Cold-atom gravimetry with a Bose-Einstein condensate*, Phys. Rev. A **84,** 033610 (2011).

[29] M. Gebbe, J.-N. Siemß, M. Gersemann, H. Müntinga, S. Herrmann, C. Lämmerzahl, H. Ahlers, N. Gaaloul, C. Schubert, K. Hammerer, S. Abend, and E. M. Rasel, *Twin-lattice atom interferometry*, Nat. Commun. **12,** 2544 (2021).

[30] S. S. Szigeti, S. P. Nolan, J. D. Close, and S. A. Haine, *High-precision quantum-enhanced gravimetry with a Bose-Einstein condensate*, Phys. Rev. Lett. **125,** 100402 (2020).

[31] R. Corgier, N. Gaaloul, A. Smerzi, and L. Pezzè, *Delta-kick squeezing*, Phys. Rev. Lett. **127,** 183401 (2021).

[32] C. D. Hamley, C. S. Gerving, T. M. Hoang, E. M. Bookjans, and M. S. Chapman, *Spin-nematic squeezed vacuum in a quantum gas*, Nat. Phys. **8,** 305 (2012).

[33] J. Peise, I. Kruse, K. Lange, B. Lücke, L. Pezzè, J. Arlt, W. Ertmer, K. Hammerer, L. Santos, A. Smerzi, and C. Klempt, *Satisfying the Einstein-Podolsky-Rosen criterion with massive particles*, Nat. Commun. **6,** 8984 (2015).

[34] I. Kruse, K. Lange, J. Peise, B. Lücke, L. Pezzè, J. Arlt, W. Ertmer, C. Lisdat, L. Santos, A. Smerzi, and C. Klempt, *Improvement of an atomic clock using squeezed vacuum*, Phys. Rev. Lett. **117,** 143004 (2016).

[35] H. Ammann and N. Christensen, *Delta kick cooling: A new method for cooling atoms*, Phys. Rev. Lett. **78,** 2088 (1997).

[36] P. Kunkel, M. Prüfer, S. Lannig, R. Rosa-Medina, A. Bonnin, M. Gärttner, H. Strobel, and M. K. Oberthaler, *Simultaneous readout of noncommuting collective spin observables beyond the standard quantum limit*, Phys. Rev. Lett. **123,** 063603 (2019).

[37] See Supplemental Material at http://link.aps.org/supplemental/10.1103/PhysRevX.15.011029 for additional information on the experimental setup, a theoretical description of the prepared squeezed state, and a theoretical determination of the scale factors, which contains Refs. [23,38–43].

[38] B. Meyer-Hoppe, M. Baron, C. Cassens, F. Anders, A. Idel, J. Peise, and C. Klempt, *Dynamical low-noise microwave source for cold-atom experiments*, Rev. Sci. Instrum. **94,** 074705 (2023).

[39] B. Fang, N. Mielec, D. Savoie, M. Altorio, A. Landragin, and R. Geiger, *Improving the phase response of an atom interferometer by means of temporal pulse shaping*, New J. Phys. **20,** 023020 (2018).

[40] G. Reinaudi, T. Lahaye, Z. Wang, and D. Guéry-Odelin, *Strong saturation absorption imaging of dense clouds of ultracold atoms*, Opt. Lett. **32,** 3143 (2007).

[41] B. Lücke, M. Scherer, J. Kruse, L. Pezzé, F. Deuretzbacher, P. Hyllus, O. Topic, J. Peise, W. Ertmer, J. Arlt, L. Santos, A. Smerzi, and C. Klempt, *Twin matter waves for interferometry beyond the classical limit*, Science **334,** 773 (2011).

[42] B. Lücke, J. Peise, G. Vitagliano, J. Arlt, L. Santos, G. Tóth, and C. Klempt, *Detecting multiparticle entanglement of Dicke states*, Phys. Rev. Lett. **112,** 155304 (2014).

[43] Y. Kawaguchi and M. Ueda, *Spinor Bose-Einstein condensates*, Phys. Rep. **520,** 253 (2012).

[44] J. M. Hartwig, *Analyse eines atomaren gravimeters hinsichtlich eines quantentests des äquivalenzprinzips*, Ph. D. thesis, Gottfried Wilhelm Leibniz Universität Hannover, 2013.

[45] W. Riley and D. Howe, *Handbook of Frequency Stability Analysis* (National Institute of Standards and Technology, Gaithersburg, MD, 2008).

[46] A. Peters, K. Y. Chung, and S. Chu, *Measurement of gravitational acceleration by dropping atoms*, Nature (London) **400,** 849 (1999).

[47] A. Lezeik, D. Tell, K. Zipfel, V. Gupta, É. Wodey, E. Rasel, C. Schubert, and D. Schlippert, *Understanding the gravitational and magnetic environment of a very long baseline atom interferometer*, arXiv:2209.08886.

[48] C. Lotz, T. Froböse, A. Wanner, L. Overmeyer, and W. Ertmer, *Einstein-Elevator: A new facility for research from μg to 5g*, Gravit. Space Res. **5,** 11 (2017).

[49] O. Anton *et al.*, *INTENTAS—An entanglement-enhanced atomic sensor for microgravity*, arXiv:2409.01051.

[50] L. Morel, Z. Yao, P. Cladé, and S. Guellati-Khélifa, *Determination of the fine-structure constant with an accuracy of 81 parts per trillion*, Nature (London) **588,** 61 (2020).

[51] J. B. Fixler, G. T. Foster, J. M. McGuirk, and M. A. Kasevich, *Atom interferometer measurement of the Newtonian constant of gravity*, Science **315**, 74 (2007).

[52] G. Rosi, F. Sorrentino, L. Cacciapuoti, M. Prevedelli, and G. M. Tino, *Precision measurement of the Newtonian gravitational constant using cold atoms*, Nature (London) **510**, 518 (2014).

[53] B. Schrinski, P. Haslinger, J. Schmiedmayer, K. Hornberger, and S. Nimmrichter, *Testing collapse models with Bose-Einstein-condensate interferometry*, Phys. Rev. A **107**, 043320 (2023).

[54] C. Cassess, B. Meyer-Hoppe, E. Rasel, and C. Klempt, supporting data, 10.25835/VCCCUUHF.